

## Photoemission and high-resolution electron-energy-loss spectroscopy studies of CO chemisorption on thin Pd films on Au(111)

X. Y. Shen,\* D. J. Frankel, G. J. Lapeyre, and R. J. Smith

*Physics Department, Montana State University, Bozeman, Montana 59717*

(Received 10 September 1985)

We present experimental observations of CO chemisorption on thin epitaxial Pd films on Au(111) using high-resolution electron-energy-loss spectroscopy (HREELS) and ultraviolet photoemission spectroscopy (UPS). The results confirm earlier UPS studies which show that a supported Pd monolayer exhibits weak CO chemisorption. We associate this behavior with the filling of the Pd  $d$  states and a reduced occupation of the molecular  $2\pi^*$  CO orbital. Consistent with this picture for the Pd monolayer is our HREELS observation of a weak, broadened loss peak for the C—O stretching mode which we attribute to two different adsorption sites: one site on the Pd monolayer with increased stretching frequency due to reduced CO  $2\pi^*$  occupation, and one site associated with defects in the thin Pd film. For thick Pd overlayers, a coverage-dependent shift in the C—O stretching frequency is observed.

### I. INTRODUCTION

There is at the present time considerable interest in the modification of the physical and chemical properties of solid surfaces, particularly in the area of supported thin films. The chemisorption of CO on Pd surfaces is a typical example for which it has been shown<sup>1-5</sup> that while bulk Pd surfaces strongly chemisorb CO, monolayer-thick films weakly chemisorb CO similar to the case of CO on noble metals. For example, recent photoemission studies of the adsorption of CO on a Ta(110)-supported Pd monolayer at liquid-nitrogen temperature indicate<sup>4</sup> that the  $1\pi$  and  $5\sigma$  molecular orbitals of CO appear to reverse their relative binding energies, showing a reduced  $5\sigma$  binding energy as compared with that on the bulk Pd(111) surface. A shake-up satellite associated with the photoexcitation of the  $4\sigma$  molecular orbital is also observed. Such a satellite is not observed for CO chemisorption on bulk Pd(111), but is observed for the weak chemisorption system of CO on Cu(111).<sup>6</sup> These satellites can be explained if there is a reduced occupation of the  $2\pi^*$  antibonding orbital for CO on the noble metal, resulting in a reduced ability to effectively screen the  $4\sigma$  core hole following photoexcitation.<sup>7,8</sup> In the present investigation we have been able to monitor the transition from weak to strong chemisorption as a function of Pd film thickness using high-resolution electron-energy-loss spectroscopy (HREELS) and ultraviolet photoemission spectroscopy (UPS).

In an attempt to better understand the modified electronic properties of the supported Pd monolayer, we have been studying thin films of Pd on Au(111).<sup>3,9</sup> These studies differ from those on W(110) (Ref. 1), Nb(110) (Ref. 2), Ta(110) (Ref. 4), and Mo(110) (Ref. 5) in two important respects. First, since both Pd and Au are fcc metals with a lattice mismatch of only 4%, the epitaxial growth of the Pd overlayer is subject to very different strains as compared to the distortion required for growth on the (110) bcc substrates. Second, since the density of states near the Fermi energy  $E_F$  is expected to play an important role in

the chemisorption process,<sup>10</sup> it is valuable to examine directly the changes in the density of states for the Pd overlayer. This is greatly facilitated for Pd on Au since the contribution to the photoemission spectrum from the substrate  $d$  bands is energetically removed from the region of interest ( $E_F$ ) in contrast to the bcc metals mentioned above.

Previous photoemission studies in our laboratory showed that for the Pd monolayer on Au(111) the density of states near  $E_F$  is relatively small as compared with that for multilayer and bulk Pd, and that the Pd monolayer exhibits inert behavior with respect to CO chemisorption. For the Pd monolayer, the Pd  $d$  levels are filled and about 1 eV below  $E_F$ , very similar to the noble metal, Cu. This lowering of the  $d$  levels is expected to reduce the amount of charge transfer to the CO  $2\pi^*$  molecular orbital, and thus lead to a weaker chemisorption bond.<sup>7,8</sup> In the present work, we have applied HREELS in conjunction with photoemission to investigate the bonding of CO to Pd monolayers. HREELS provides information complementary to that obtained in our earlier work. We have observed that the C—O stretching-mode loss peak on the Pd monolayer has a shoulder on the high loss-energy side, while the loss peak of multilayer films is not appreciably broadened. We show, using a model for multisite absorption on thin Pd films, that this observation is consistent with a picture of reduced  $2\pi^*$  back bonding on the Pd monolayer.

### II. EXPERIMENTAL

The experiments were performed at the Center for Research in Surface Science and Submicron Analysis (CRISS) facility at Montana State University, using a Leybold-Heraeus system equipped with instrumentation for HREELS, UPS, x-ray photoemission spectroscopy (XPS), low-energy electron diffraction (LEED), and residual gas analysis (RGA). The HREELS apparatus was typically operated with 6.5-eV primary electron energy

and a resolution on the elastic peak of  $(13 \pm 0.5)$ -meV full width at half maximum (FWHM). Counting rates on the elastic peak for clean Pd(111) films were between 1 and  $2 \times 10^4$  counts/sec. The UPS measurements were performed using a He resonance lamp and the Leybold-Heraeus EA-11 hemispherical analyzer, operating at a pass energy of 25 eV, and angular acceptance of  $6^\circ$ . The pressure in the sample chamber during the experiments was typically  $3 \times 10^{-10}$  Torr.

A clean Au(111) surface was prepared using a 3-mm-thick by 6-mm-diam button cut from a single-crystal Au rod. After chemical etching, the button was inserted into the vacuum chamber and further cleaned with sputter-annealing cycles. The Pd films of different thicknesses were evaporated from a directly-heated coil of Pd foil stretched between Ta support rods. This evaporator allowed us to maintain a pressure of  $5 \times 10^{-10}$  Torr during film deposition, and to achieve Pd films relatively free of CO contamination immediately after deposition, unlike the problems in our earlier work.<sup>3</sup> The Au(111) substrate was at room temperature during film deposition. The thickness of each film and the rate of deposition were monitored using a quartz-crystal oscillator (QCO). Film-thickness calibration was accomplished using the attenuation of the Au 4*p* core level and the growth of the Pd 3*p* core level in the XPS spectra. XPS measurements in which the takeoff angle from the Pd monolayer was varied showed that the intensity of the Pd 330-eV Auger line was approximately isotropic as a function of polar angle, indicating that interdiffusion between surface Pd and subsurface Au atoms was probably not taking place,<sup>11</sup> consistent with our previous Auger analysis.<sup>3</sup> Based on the above considerations, we estimate that the uncertainty in our Pd film thicknesses is less than  $\pm 20\%$ , with the main contribution to this uncertainty coming from the uncertainty in the mean free path for electrons with 940-eV kinetic energy. LEED patterns with  $(1 \times 1)$  sixfold symmetry were observed for each epitaxial Pd(111) film. After the LEED and XPS measurements used to characterize each deposited Pd film, the UPS and HREELS spectra were recorded as described in the next section.

For the CO chemisorption studies, Pd films of different thicknesses were exposed to various amounts of CO until saturation of the CO-induced signal intensity was achieved. We used UPS to monitor the CO-derived features originating from the  $5\sigma + 1\pi$  and  $4\sigma$  molecular orbitals, and HREELS to measure the C—O stretching frequency.

### III. RESULTS

#### A. UPS studies

In Fig. 1 we show the valence-band portion of the photoemission spectra obtained in normal emission using HeII radiation. The curves are plotted as a function of initial-state energy with the zero of energy at the Fermi level ( $E_F$ ). The unpolarized light was incident at an angle of  $45^\circ$  from the surface normal. The thickness in monolayers (ML) of the Pd overlayer as determined from the attenuation of the substrate 4*p* core-level emission is indicated on the left-hand side of the figure. In comparing

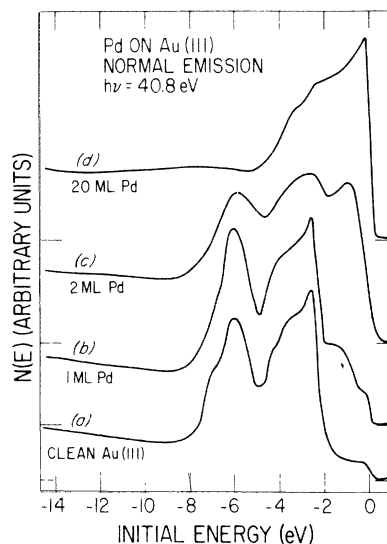


FIG. 1. Angle-resolved photoemission spectra collected normal to the surface and plotted as a function of initial-state energy below the Fermi energy ( $E_F = 0$ ) for (a) clean Au(111) and (b)–(d) thin epitaxial Pd films. The Pd film thickness is indicated in monolayers (ML) at the left.

these results with our earlier work,<sup>3</sup> there are several important observations. First, the improved resolution with the current spectrometer allows us to clearly distinguish the step at the Fermi level for the clean Au(111) spectrum (curve *a*). Second, for the 1-ML Pd film (curve *b*), we see a distinct kink at the onset of the Pd *d*-band emission, approximately 0.5 eV below  $E_F$ . Finally, with the reduced background pressure during evaporation we are able to confirm that the lowering in energy of the Pd *d* states for the monolayer is clearly associated with the properties of the clean surface since negligible CO contamination is observed in the present results. At the highest Pd film thickness shown here, about 20 ML in curve *d*, the UPS spectrum shows *d*-band structure very similar to that obtained from bulk single-crystal Pd(111).<sup>12</sup>

The photoemission spectrum for each Pd film was also measured as a function of CO exposure. In Fig. 2 the bottom curve is again the spectrum for a clean Au(111) surface (not exposed to CO). Curves *b* through *d* are from Pd films exposed to a near-saturation coverage of CO. We note that curve *d*, for the thick Pd film, shows the usual double-peak structure attributed to molecular CO adsorption, with the  $4\sigma$  molecular orbital at  $-10.6$  eV and the  $5\sigma + 1\pi$  molecular orbitals at  $-7.8$  eV. In marked contrast to this observation, curve *b* for the Pd monolayer shows negligible CO-derived features and only slight changes in the *d*-band region even after a total exposure to more than 100 L of CO (1 L =  $1 \times 10^{-6}$  Torrsec). For the 2-ML Pd film in curve *c*, the CO-derived features are relatively weak following a saturation exposure of about 20 L. For the thick Pd film in curve *d*, 1.5 L of CO is enough to achieve saturation intensity for the CO molecular orbitals.

These results with improved energy resolution confirm our previous conclusions<sup>3</sup> and show more clearly that (1)

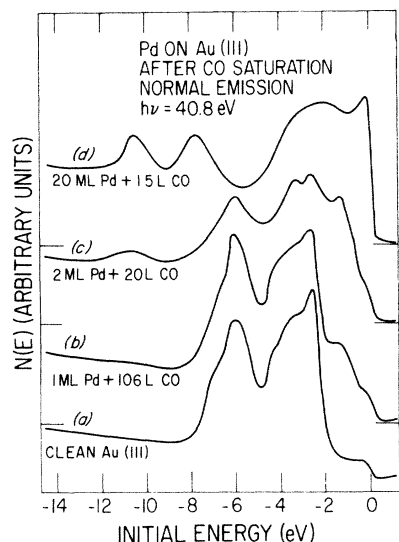


FIG. 2. Angle-resolved photoemission spectra for the same Pd films as shown in Fig. 1, measured after exposing the surfaces to a near-saturation coverage of CO. The exposure used for each film is indicated at the left in langmuirs (L).

the density of states near the Fermi energy is relatively small for the supported Pd monolayer as compared with that for the multilayer and bulk Pd surfaces, and (2) the supported Pd monolayer apparently chemisorbs very little CO in marked contrast to the behavior observed for CO on bulk Pd, and on thick Pd films.

### B. HREELS studies

Following deposition of each Pd film the electron-energy-loss spectrum was also recorded. The dominant loss feature observed was the C—O stretching mode in the region of 226–240 meV ( $1823$ – $1936$   $\text{cm}^{-1}$ ), depending on CO coverage and Pd film thickness. In Fig. 3 we show the HREELS spectra for three Pd films exposed to a near-saturation coverage of CO. The C—O stretching-mode loss peak for the 1-ML Pd film (curve *a*) is centered at  $231 \pm 2$  meV ( $1863$   $\text{cm}^{-1}$ ) and is very weak due to the low CO coverage. To improve the signal-to-noise level for this feature we scanned the region of interest around the C—O stretching mode with increased dwell time per channel ( $\times 4$ ), and show the results of this slow scan in Fig. 3. The results for the 20-ML Pd film after exposure to a

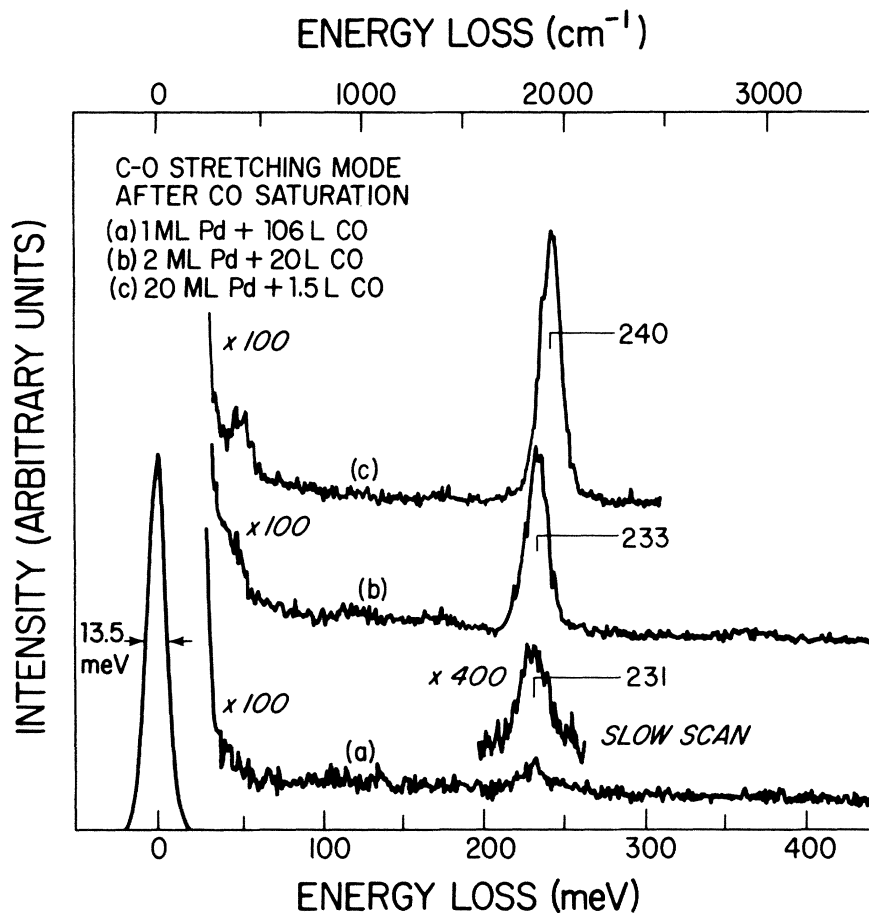


FIG. 3. HREELS spectra for thin Pd films on Au(111) after near-saturation exposure to CO. Film thickness and CO exposure are shown at the top. The curves have been normalized to the height of the elastic peak of curve *a*. Counting rates (counts/sec) at the elastic peak were (a)  $1.3 \times 10^4$ , (b)  $1.2 \times 10^4$ , and (c)  $1.8 \times 10^4$ .

near-saturation coverage of CO (curve *c*) show the C—O stretching mode at  $240 \pm 1$  meV ( $1936 \text{ cm}^{-1}$ ) with a width of 16 meV. The carbon-metal stretching mode is present at  $46 \pm 2$  meV. We observed that the CO adsorption had a negligible effect on the width of the elastic peaks ( $13.0 \pm 0.5$  meV), although adsorption of CO did affect the height of the elastic peaks considerably. For the 1-ML Pd overlayer, the initial adsorption of 1 L of CO reduced the elastic peak intensity from  $1.6 \times 10^4$  to  $1.3 \times 10^4$  counts/sec. Further CO exposures did not change the shape or size of the elastic peak. For the thick Pd overlayers, CO adsorption increased the elastic peak intensity by nearly 50% for some films while leaving the width essentially unchanged.

Estimates of CO coverage on the Pd films can be obtained by assuming a saturation CO coverage on the thick Pd films of 0.5 ML and then assuming that the normalized C—O stretching-mode peak area is proportional to CO coverage. Using these assumptions, we find that the CO coverage on the as-prepared 20-ML Pd film is less than 0.05 ML, i.e., less than 10% of the saturated coverage peak area. This estimate is consistent with the coverage expected from exposure to the residual gas if we assume a unity sticking coefficient for CO on Pd, and also with the absence of discernible CO features in the UPS spectra of the as-prepared Pd film (curve *d*, Fig. 1). Similarly, the CO coverage on the CO-saturated monolayer Pd film is less than 10% of the saturated thick-film CO peak area, and coverage on the as-prepared monolayer film is slightly less. These estimates of CO coverage for the Pd monolayer are again consistent with the absence of CO-derived features in the UPS spectra (curve *b* in Figs. 1 and 2).

The width and loss energy for the C—O stretching mode were measured as a function of CO exposure. For the thick Pd film, a relatively low intensity loss peak was observed at  $226 \pm 1$  meV ( $1823 \text{ cm}^{-1}$ ) immediately following film deposition. As noted above, the initial area of this loss peak at 226 meV corresponded to a CO coverage of approximately 0.05 ML. As the thick Pd film was exposed to additional CO, the stretching-mode loss peak increased in intensity and gradually shifted to higher loss energy. Approximately 1.5 L of CO was sufficient to saturate the intensity of the CO loss peak for the thick Pd film, leading to the spectrum shown in Fig. 3, curve *c*. These results are summarized in Fig. 4(b), where we plot the position of the center of the C—O stretch-mode loss peak as a function of CO exposure in langmuirs for both the thick Pd film (20 ML) and the Pd monolayer. The solid lines in Fig. 4(b) are provided merely to guide the eye and to distinguish between the two separate sets of data. For comparison, we show in Fig. 4(a) the more-detailed measurements of the coverage-dependent frequency shift for the C—O stretching mode observed in previous infrared (ir) studies of CO on bulk Pd(111).<sup>13,14</sup> It can be seen that our results for the frequency shift on the 20-ML film fall within the range of and are consistent with the range of frequencies observed in the ir studies. The abrupt shift in the ir frequency beginning at a coverage of approximately 0.33 ML was attributed to a change in the CO bonding site, from a threefold bridge at coverages up

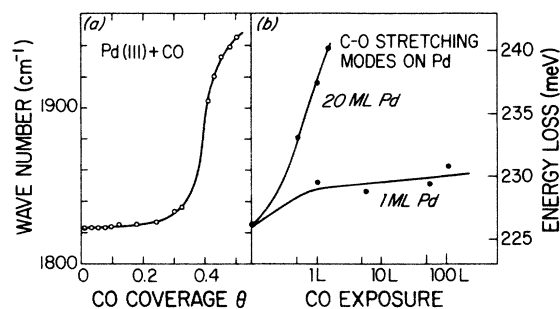


FIG. 4. (a) Coverage dependence of the IR absorption frequency for the C—O stretching mode on Pd(111) at room temperature, from Refs. 13 and 14, used with permission. (b) Exposure dependence of the center of the HREELS loss peak for the C—O stretching mode on thin Pd films on Au(111).

to 0.33 ML to a twofold bridge for the higher coverages. In our studies we did not independently measure the CO coverage, nor did we observe any CO-induced LEED patterns.

The C—O stretching frequency has a much weaker exposure-dependent shift for CO on the Pd monolayer, as seen in Fig. 4(b). Exposure only to the residual gas leads again to a low intensity loss feature centered at 226 meV immediately following film deposition. We note again that this coverage of CO represents at most a coverage of 10% of the thick-film saturation CO coverage, or approximately 0.05 ML. After an exposure of 1 L of CO, the C—O stretching frequency has shifted to 230 meV ( $1855 \text{ cm}^{-1}$ ) and increases slightly in width. With an additional 100 L of CO exposure, the C—O loss feature shifts to  $231 \pm 2$  meV ( $1863 \text{ cm}^{-1}$ ), the intensity increases slightly, and the peak width has increased to 21 meV.

#### IV. DISCUSSION

For the UPS results presented here, and in our earlier work, we have made the suggestion that the inert behavior with respect to CO chemisorption for the Pd monolayer on Au(111) is connected with the reduced density of states at the Fermi energy. It is clear from our present HREELS results, and from the low-temperature measurements of Ruckman *et al.*,<sup>4</sup> that the Pd monolayer is not totally inert to CO chemisorption, but that this surface exhibits weak CO chemisorption. The appearance of a shake-up satellite in the low-temperature UPS is an indicator of the weak character of the surface CO bond,<sup>7</sup> and can be associated with reduced occupation of the antibonding  $2\pi^*$  molecular orbital.<sup>7,15</sup> Since the  $2\pi^*$  orbital has significant antibonding character, one might expect that a reduction in the occupation of this orbital would lead to an increase in the C—O stretching frequency as the bond becomes more stiff, approaching closer to the gas-phase limit. On the other hand, changes in the bonding site can also result in frequency shifts for the C—O stretch.<sup>13,14</sup>

If one attributes the shift in the C—O stretching frequency to coverage dependence only, as observed in the ir results for bulk Pd(111), there is an apparent contradic-

tion in our results for the Pd monolayer. The apparent frequency shift for CO on the Pd monolayer, based simply on the peak position, is about 5 meV ( $43\text{ cm}^{-1}$ ), reaching  $231\text{ meV}$  ( $1855\text{ cm}^{-1}$ ), corresponding to a CO coverage of approximately 0.38 ML in the data of Fig. 4(a). Such a high CO coverage should be readily apparent in the UPS results for the Pd monolayer, but in Fig. 2(b) we see no significant emission from the CO orbitals. For this reason we have considered other mechanisms for the apparent frequency shift and increased width of the C—O loss peak on the Pd monolayer.

In Fig. 5 we show the loss peak for the C—O stretching mode on the Pd monolayer immediately after film deposi-

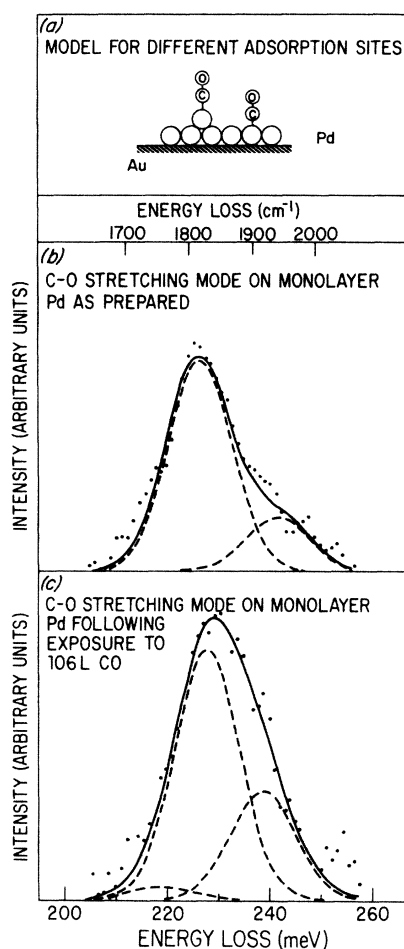


FIG. 5. Decomposition of the HREELS loss peaks for CO adsorbed on a Au-supported Pd monolayer. The dashed curve at higher energy is assigned to weakly chemisorbed CO on the Pd monolayer, and the dashed curve at lower energy to strongly chemisorbed CO at multilayer defects in the thin Pd film, as sketched in the top panel. The solid curves are the sums of the respective sets of dashed curves. A five-point smoothing has been applied to the experimental data [points in (b) and (c)]. The data have not been normalized to the elastic peak. (b) C—O stretch on the Pd monolayer as-prepared; elastic peak height is  $1.6 \times 10^4$  counts/sec. (c) C—O stretch on the Pd monolayer after 106 L of CO exposure; elastic peak height is  $1.3 \times 10^4$  counts/sec.

tion [points in Fig. 5(b)], and for the same film after an exposure to 106 L of CO [points in Fig. 5(c)]. The points in Figs. 5(b) and 5(c) are the original data points after background subtraction and one five-point smoothing to remove some of the noise seen in Fig. 3. Since the FWHM for the curves in Fig. 5 was about 21 meV, while the FWHM for the elastic peak remained at 13 meV, and the FWHM for the CO loss peaks on thick films was only 16 meV, we used a curve-fitting program to fit the loss peaks with a sum of two or more Gaussian-shaped peaks of equal width. The results of this analysis are shown as the dashed curves in Fig. 5. The solid curve in each panel is the sum of the dashed curves and represents a reasonably good fit to the experimental points. A main peak was centered at 226 meV with a secondary peak centered near 240 meV. The widths were determined to be about 15 meV, which is reasonably close to the 16 meV width for loss peaks on the thick Pd films. A similar analysis was carried out for five spectra: the Pd monolayer as-prepared, and the Pd monolayer following CO exposures of 1, 6, 56, and 106 L. The average values for the two peak positions were  $226 \pm 2\text{ meV}$  ( $1823\text{ cm}^{-1}$ ) and  $238 \pm 2\text{ meV}$  ( $1919\text{ cm}^{-1}$ ), respectively, with equal widths of  $15 \pm 1\text{ meV}$ . The experimental points in Fig. 5 have not been normalized to the elastic peak, which decreased slightly with CO exposure. A final comment with respect to the curve fitting concerns the quality of fit. A "good" fit was determined by several factors, including a reasonable FWHM for the component peaks, and a low chi-square value for the fit. In most cases a fit with only two Gaussian peaks seemed quite satisfactory for loss peaks on the Pd monolayer although the chi-square value could be reduced at times with the addition of a third peak as shown in Fig. 5(c). Since the area of this third peak was only a few percent of the total area, no physical significance was assigned to this peak. For CO loss peaks on thick Pd films, as in Fig. 3, a single Gaussian was adequate to give a satisfactory fit.

The decomposition of the CO loss peaks as described above makes sense in the following model for the Pd monolayer. As shown in Fig. 5(a), it is quite likely that we have some defects in the Pd monolayer, in the form of atomic-size islands two or more atoms thick. This seems even more likely when one recalls that as a precaution against interdiffusion we did not anneal the film after deposition. Also, with the  $\pm 20\%$  uncertainty in our film thickness as discussed earlier, there is a good chance for some second-layer Pd atoms in these results. Based on our results for the thick Pd film, and the ir results, these defects would present an adsorption site with a relatively high sticking probability, and should immediately strongly chemisorb a CO molecule with the corresponding low-coverage, thick-film C—O stretching mode at 226 meV. Thus the defect sites will fill up quickly, while the monolayer sites, with a tendency for weak chemisorption, will have a much lower equilibrium coverage at room temperature, and a correspondingly lower loss-peak intensity. We tentatively assign the peak at 238 meV to the stretching mode of CO on the Pd monolayer. This picture is then consistent with the UPS results in that, even with 106-L exposure, we still have such a small CO coverage

that the CO orbitals are not visible in the UPS, unless one cools the sample to low temperature to decrease the desorption probability.<sup>4</sup>

The higher stretching frequency which we attribute to CO on the Pd monolayer can be explained using the model of weak chemisorption. Reduced metal-to-CO backbonding lowers the occupancy of the  $2\pi^*$  orbital and results in an increase in the CO stretching frequency since the  $2\pi^*$  orbital has a predominantly antibonding character. Reduced back bonding is also consistent with our UPS observation of reduced  $d$ -band density at the Fermi energy; i.e., formation of the Pd monolayer increases the energy gap between the empty  $2\pi^*$  orbital and the filled Pd  $d$  states, with a subsequent decrease in the hybridization, or charge transfer. An alternative explanation for the higher stretching frequency on the monolayer is a different bonding site for CO on the monolayer. It is well documented<sup>14</sup> that a shift from a threefold bridge site to a twofold bridge site can lead to an increase in the C—O stretching frequency. The magnitude of the difference observed here, 226 meV versus 238 meV, is consistent with the qualitative picture, wherein the stretching frequency decreases as ligancy of the metal—CO bond increases. Of course, these two phenomena may not be exclusive of each other since a change in the preferred bonding site, from the threefold to the twofold bridge position, might also be accompanied by a decrease in the amount of charge transfer to the antibonding  $2\pi^*$  orbital.<sup>14</sup> We note, however, that our value for a loss peak at 238 meV for the Pd monolayer is considerably below the value of 257 meV observed for weak chemisorption of CO on Cu(111),<sup>7</sup> and could represent a case of intermediate strength for the chemisorption bond. Finally, we have not considered in detail the possibility that the higher stretching frequency observed for CO on the Pd monolayer might result from a change in the orientation of the molecule on the monolayer, e.g., side bonded.

In conclusion, we have measured the behavior of CO

chemisorbed on thin Pd films grown epitaxially on Au(111) using HREELS and UPS. We believe that CO exhibits weak chemisorption properties on the Pd monolayer, characterized by the satellite structure in low-temperature photoemission and by an increase in the C—O stretching frequency due to reduced back bonding to the  $2\pi^*$  molecular orbital. We have interpreted the broadened loss peak for CO on a Au-supported Pd monolayer as being due to the sum of two loss peaks, at approximately 226 and 238 meV. These peaks are tentatively associated with CO on a small number of multilayer-type defect sites in the Pd monolayer (226 meV), and with the loss energy for CO weakly chemisorbed at low coverage on the Pd monolayer (238 meV). Additional theoretical and experimental work is needed to confirm whether or not this shift to higher frequency is associated with a change in bonding site from a threefold to a twofold bridge position. It would certainly be beneficial in future experiments on such supported thin films, to carry out in one experimental chamber the HREELS and the low-temperature photoemission measurements. If possible, XPS measurements of the carbon  $1s$  core level should also be included to check for the presence of shake-up satellites.

#### ACKNOWLEDGMENTS

We would like to acknowledge the assistance of M. Jaehnig and T. Jungst, and useful discussions with J. Hermanson, J. Anderson, and W. Ford. We thank H. Farrell for use of the Au(111) crystal. This work was supported by the National Science Foundation (NSF) through Grants No. DMR 84-01196 and No. DMR 82-05581, and through the NSF-supported Montanans On a New Trac for Science (MONTS) program on Grant No. ISP 80-11449. Measurements were performed at CRISS, a NSF Regional Instrumentation User Facility sponsored under NSF Grant No. DMR 82-09640.

\*Permanent address: Beijing Normal University, People's Republic of China.

<sup>1</sup>D. Prigge, W. Schlenk, and E. Bauer, *Surf. Sci.* **123**, L698 (1982).

<sup>2</sup>M. W. Ruckman and M. Strongin, *Phys. Rev. B* **29**, 7105 (1984).

<sup>3</sup>X. Y. Shen, D. J. Frankel, J. C. Hermanson, G. J. Lapeyre, and R. J. Smith, *Phys. Rev. B* **32**, 2120 (1985).

<sup>4</sup>M. W. Ruckman, P. D. Johnson, and M. Strongin, *Phys. Rev. B* **31**, 3405 (1985).

<sup>5</sup>H. Poppa and F. Soria, *Phys. Rev. B* **27**, 5166 (1983).

<sup>6</sup>C. L. Allyn, T. Gustaffson, and E. W. Plummer, *Solid State Commun.* **24**, 531 (1977).

<sup>7</sup>D. Heskett, E. W. Plummer, and R. P. Messmer, *Surf. Sci.* **139**, 558 (1984).

<sup>8</sup>H.-J. Freund and E. W. Plummer, *Phys. Rev. B* **23**, 4859 (1981).

<sup>9</sup>X. Y. Shen, D. J. Frankel, J. Hermanson, G. J. Lapeyre, and R. J. Smith, in *Thin Films: The Relationship of Structure to Properties*, edited by K. S. SreeHarsha and C. R. Aita, Proceedings of the Materials Research Society, Vol. 47 (North-Holland, New York, 1985).

<sup>10</sup>P. J. Feibelman and D. R. Hamann, *Phys. Rev. Lett.* **52**, 61 (1984).

<sup>11</sup>W. F. Egelhoff, Jr., *J. Vac. Sci. Technol. A* **3**, 1511 (1985).

<sup>12</sup>D. R. Lloyd, C. M. Quinn, and N. V. Richardson, *Solid State Commun.* **20**, 409 (1976).

<sup>13</sup>A. M. Bradshaw and F. M. Hoffman, *Surf. Sci.* **72**, 513 (1978).

<sup>14</sup>H. Ibach and D. L. Mills, *Electron Energy Loss Spectroscopy and Surface Vibrations* (Academic, New York, 1982), p. 284ff.

<sup>15</sup>R. P. Messmer, S. H. Lamson, and D. R. Salahub, *Phys. Rev. B* **25**, 3576 (1982).